

Incoherent spatial solitons in effectively instantaneous nonlinear media

CARMEL ROTSCCHILD¹, TAL SCHWARTZ¹, OREN COHEN^{1,2} AND MORDECHAI SEGEV^{1*}

¹Physics Department and Solid State Institute, Technion, Haifa 32000, Israel

²JILA and Department of Physics, University of Colorado at Boulder, Colorado 80309-0440, USA

*e-mail: msegev@tx.technion.ac.il

Published online: 25 May 2008; doi:10.1038/nphoton.2008.81

Incoherent optical spatial solitons are self-trapped beams with a multimodal structure that varies randomly in time. They form when their diffraction-broadening, which is governed by their spatial correlations, is balanced by nonlinear interaction between the waves and the medium, resulting in the stationary propagation of the time-averaged intensity structure of the beam. The experimental observation of incoherent solitons has opened up exciting new avenues in soliton science. However, all incoherent spatial solitons observed to date have been supported by nonlinearities with a slow response time, τ , that is much longer than the characteristic fluctuation time of the beam, $t_c \ll \tau$. Here, we demonstrate incoherent solitons in effectively instantaneous nonlocal nonlinear media where $\tau \ll t_c$. These solitons exhibit fundamentally new features (for example, propagation at random trajectories), and can be created in various optically nonlinear media, as well as in other fields where the nonlinearity is nonlocal and very fast.

Incoherent beams are multimode entities whose structures vary randomly in time. They are characterized by their correlation function, which governs their diffraction properties. Such a beam can self-trap, forming an incoherent spatial soliton, when its fluctuating structure induces a non-fragmented waveguide that guides the beam within it, robustly balancing its diffraction-broadening¹. Such a mechanism was demonstrated in 1996 with solitons made of quasi-monochromatic partially spatially incoherent light². Shortly thereafter, self-trapping of a beam emitted from an incandescent bulb was observed: a ‘white-light soliton’³. These experiments opened new directions in soliton science^{4–14}. However, all incoherent optical spatial solitons observed up to this work were supported by non-instantaneous nonlinearities, whose response time τ is much slower than the fluctuation time of the light, $t_c \ll \tau$. In this fashion, the slow response of the medium averages over the rapidly fluctuating fragmented structure of the beam, inducing a smooth non-fragmented waveguide^{2–12,15–19}. Here, we follow a recent prediction²⁰ and demonstrate experimentally incoherent solitons in effectively instantaneous nonlocal nonlinear media where $\tau \ll t_c$. In such a self-trapping mechanism, the induced waveguide is non-fragmented due to the spatial-averaging tendency of the nonlocal nonlinearity (in contrast to ‘conventional’ incoherent solitons where self-trapping involves time-averaging in spatially local nonlinear media). These effectively instantaneous incoherent solitons exhibit new features, and can be obtained in various optically nonlinear media²¹, as well as in other fields where the nonlinearity is nonlocal yet very fast.

An optically nonlinear medium is considered nonlocal when the nonlinear effect at a given location is a function of the field at some nonlocality range surrounding that location. Nonlocality plays an important role in many areas of nonlinear physics. Nonlocality typically arises from an underlying transport mechanism (heat^{22–25}, atoms in a gas²⁶, charge carriers^{19,21}, for

example), or from long-range forces (for example, electrostatic interactions in liquid crystals^{28,29}) and many-body interactions as with matter waves in Bose–Einstein condensates (BECs)^{30,31} and plasma waves^{14,32,33}. In nonlinear optics, nonlocality has been found in photorefractives²⁷, thermal nonlinear media^{22–25}, atomic vapours²⁶, liquid crystals^{28,29} and semiconductor amplifiers²¹. Interestingly, in spite of the natural spatial-widening tendency of nonlocality, even highly nonlocal nonlinearities can support solitons in their simplest (bell-shaped) realization^{26,28,29,34–36} or as multipole solitons^{37–39}. When the nonlocality range greatly exceeds the width of the beam, the induced index change has a bell-shaped-structure, which depends only on the beam power⁴⁰, and is largely insensitive to the intensity pattern²⁰.

CONCEPT

Spatially incoherent light can be modelled as a sequence of coherent multimode (speckled) beams, each occurring within a short time window t_c , and then switched abruptly to another window with a different modal distribution (speckled pattern), repeatedly⁴¹. The interaction between an incoherent beam and a nonlinear medium is considered instantaneous when the time response of the medium, τ , is much shorter than the fluctuation time of the wave, t_c . In such a case, the nonlinear medium responds to the speckled pattern in each time window, within which the beam is fully coherent. In a highly nonlocal nonlinearity, the coherent speckled beam induces, at every moment in time, a smooth (non-fragmented) waveguide, which is uniform in the direction of propagation. If the modes of the induced waveguide span the same space as the modes constructing the light, it is possible to find conditions for which all realizations of the incoherent beam (all speckled patterns whose time/ensemble average makes up the incoherent beam) are self-trapped within the waveguide that the beam induces²⁰. When this happens, each of the instantaneous

self-trapped multimode realizations (beams) does not broaden. However, each of these instantaneous self-trapped beams carries transverse momentum arising from the (random) interference among its modal constituents²⁰. When the system conserves transverse momentum, the initial transverse momentum determines the trajectory of the beam. Consequently, these instantaneous self-trapped beams are propagating in random directions. The ensemble average over multiple realizations of such self-trapped (yet randomly deflected) beams displays nonlinear broadening (statistical nonlinear diffraction)²⁰. In the limit of a large number of modes, the nonlinear diffraction of this ensemble-averaged beam becomes negligible and an incoherent soliton forms.

EXPERIMENTS

EXPERIMENTAL TECHNIQUES

We first demonstrate multimode solitons and statistical nonlinear diffraction with a simple example of a bimodal beam, highlighting the role of the relative phase between its modes. We then experiment with a highly incoherent beam generated by a diffuser and show how statistical nonlinear diffraction becomes negligible, yielding an incoherent soliton. All our experiments are carried out in lead-glass displaying a thermal nonlinearity of the self-focusing type²². The samples have square, 2×2 mm cross-sections, and 83 mm long in the propagation direction. The four transverse boundaries of the samples are thermally connected to a heat sink and maintained at room temperature.

Realizing instantaneous interactions in our thermal nonlinear medium is not straightforward. The thermal nonlinearity is slow ($\tau \sim 0.1$ s) compared with the fluctuation time of natural incoherent light. Thus, we artificially construct an incoherent beam, by dividing the fluctuating field into a sequence of temporal windows of duration t_c within which the multimode (speckled) beam structure is kept fixed, but with a random relation between the patterns in different windows. Within each time window, which is set to be much longer than the response time of the nonlinearity, the relative phases among the spatial modes are fixed. We monitor the propagation of this multimode beam after the nonlinear index change, Δn , has reached temporal steady state. Under these conditions, in each measurement we observe self-trapping of a coherent multimode beam. This is physically identical to having a multimode beam self-trapped in an instantaneous nonlinearity, and monitoring the beam at a given snapshot in time. Carrying out multiple experiments with different (random) realizations of the multimode beam and taking the ensemble average corresponds to monitoring the long-timescale behaviour of an incoherent beam. The ensemble average over many realizations of the speckled beam is in fact an artificially constructed partially spatially incoherent beam. When this ensemble-average beam exhibits (under appropriate conditions) stationary propagation, it is an incoherent soliton.

SCALAR MULTIMODE SOLUTIONS

Before proceeding, we note that, thus far, scalar (single-field) multimode solitons have never been observed in any homogeneous nonlinear media, with either a local or a nonlocal response. By multimode solitons we mean solitons that populate at least two different modes of their jointly induced potential (which forms a waveguide). The challenge with demonstrating multimode solitons is to overcome the beating between the modes, which, in a local nonlinearity, prevents the formation of a stationary waveguide. The simplest means to eliminate modal beating is by launching the two modes at different polarizations

(Manakov-type solitons). Another approach is to eliminate the contribution of the modal beating to the induced potential by launching every mode in a different field (thus creating a composite or vector soliton), with the fields varying much faster than the response time of the nonlinearity⁴². The same mechanism is what enables incoherent solitons in non-instantaneous nonlinear media². However, all of these are vector solitons (solitons comprising more than one field, hence described by several coupled wave equations) and not scalar solitons (described by a single wave equation). Because of modal beating, the observation of scalar multimode solitons has so far been elusive. Specifically in nonlocal nonlinearities, all multimode solitons that were demonstrated were either composed of multiple fields (vector solitons) or constituted a single guided mode only (for example, the scalar multipole solitons^{37–39}, which form when the beam occupies a single higher mode of its self-induced waveguide). However, as shown in ref. 20 and explained above, the nonlocal nature of the nonlinearity can keep the induced waveguide stationary even though modal beating does occur, because the induced waveguide depends only on the total power, which is a conserved quantity. The following experiments are the first to demonstrate scalar multimode solitons, taking advantage of the unique features of nonlocal nonlinearities.

EXPERIMENTS WITH BIMODAL BEAMS

The first experiment was carried out with a bimodal beam made up of modes 0 and 1 of their jointly induced potential, with the relative phase between them varying randomly from one time-window to the next. We used a laser beam of 488 nm wavelength, split it with a beamsplitter, and constructed a symmetric TEM_{00} gaussian mode in one beam, and an antisymmetric TEM_{10} mode in the other, subsequently recombining the beams with their centres coinciding. The relative phase between the beams was manipulated by reflecting the TEM_{00} beam off a mirror positioned on a step motor. Feeding the step motor with a random function such that it introduces an optical phase shift of at least 2π yields a random-phase bimodal beam. We launched this beam into the sample at normal incidence. The following experiments were repeated 50 times, with 50 random realizations of the relative phase. Typical results are shown in Fig. 1. Figure 1a and b depicts two particular realizations of the input bimodal beam, corresponding to a relative phase of $\sim\pi/2$ and $\sim3\pi/2$ between the modes, respectively. The composite input beam was $50 \times 70 \mu\text{m}$ full-width at half-maximum (FWHM). At low intensity, the input beam experienced diffraction-broadening by a factor of ~ 2.7 (Fig. 1c and d). At high intensity, each composite beam occurring within a short time window self-trapped after the thermal nonlinearity reached a temporal steady state (Fig. 1e,f). Notice that the different relative phases cause different trajectories for the self-trapped bimodal beam (Fig. 1e,f). Finally, we examined the ensemble average over 50 random realizations of the relative phase. The ensemble-average input beam has a ‘figure of 8’ structure (Fig. 1g), which is a two-dimensional (2D) generalization of the double-humped 1D structure²⁰. At low intensity, the ensemble-average beam broadened considerably (Fig. 1h). At high intensity, the ensemble-average beam narrowed down but exhibited statistical nonlinear diffraction (Fig. 1i). Comparing Fig. 1h and Fig. 1i reveals that the maxima of the low and high power output beams coincide, although at high power the humps are narrow as a consequence of the self-trapping.

We proceeded with a bimodal beam composed of the non-consecutive modes 0 and 2. To generate mode 2, we introduced two

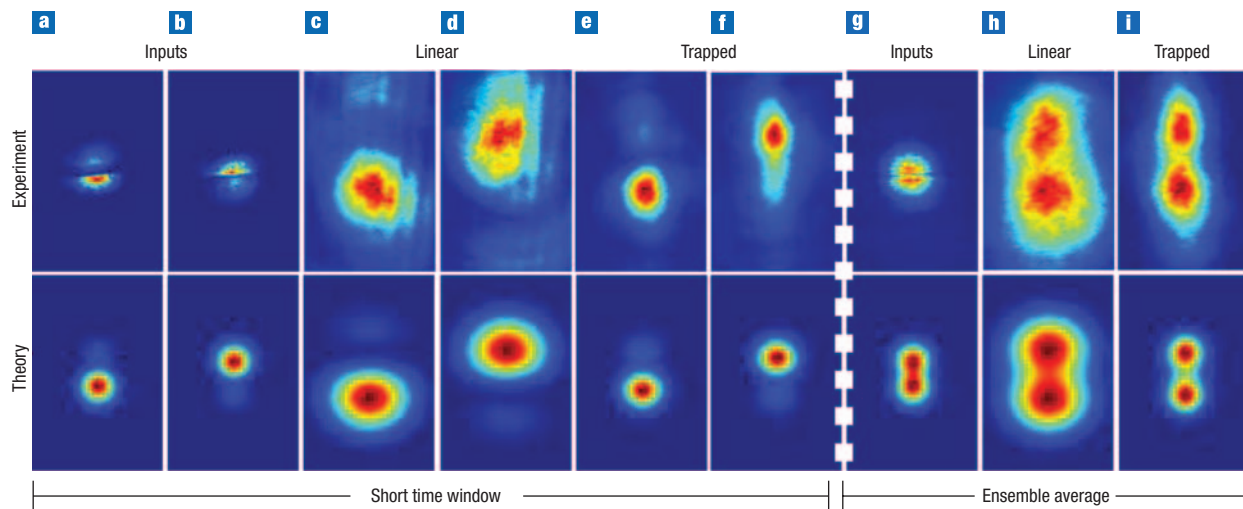


Figure 1 Self-trapping of bimodal beams composed of consecutive modes. Experimental (upper row), and theoretical (lower row) results showing self-trapped bimodal beams composed of the consecutive 0 and 1 modes. **a–f**, Two particular realizations of the relative phase between the modes. The bimodal input beams (**a,b**) linearly diffract at low power (**c,d**). At high power each beam self-traps with a trajectory that depends on the initial relative phase (**e,f**). The ensemble-average input beam (**g**) linearly diffracts at low power (**h**), whereas at high power it displays statistical nonlinear diffraction (**i**). The dimensions of these plots are $550 \mu\text{m} \times 370 \mu\text{m}$.

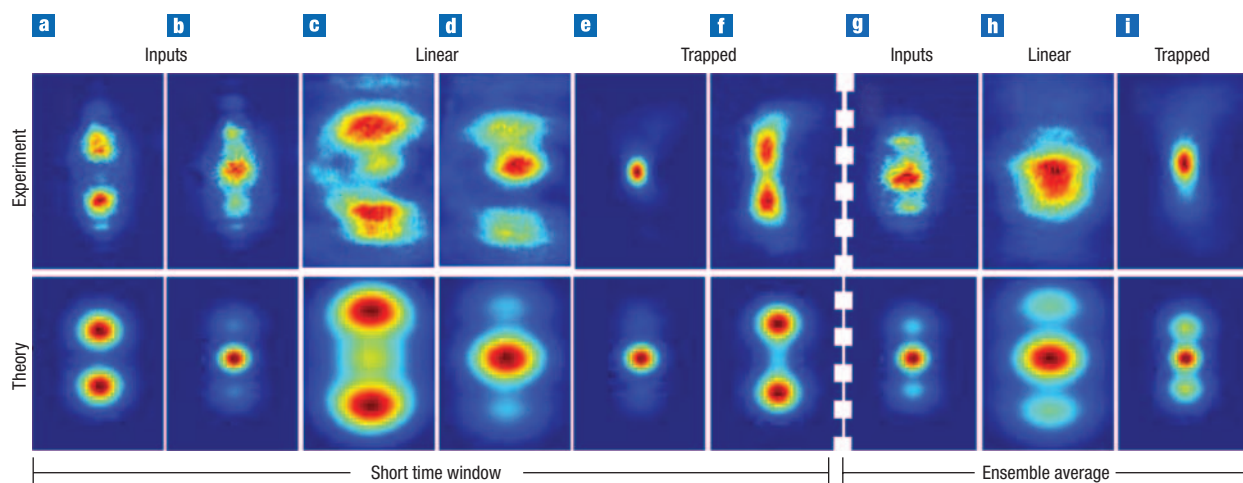


Figure 2 Self-trapping of bimodal beams composed of non-consecutive modes. Same arrangements as in Fig. 1, but for self-trapped bimodal beams composed of the non-consecutive modes 0 and 2. The trajectory of the instantaneous self-trapped beam is always on-axis, so the ensemble-average beam forms an incoherent soliton, without statistical nonlinear diffraction (**i**). The dimensions of these plots are $550 \mu\text{m} \times 370 \mu\text{m}$.

evenly spaced, π -phase jumps across the beam. Figure 2 shows typical results obtained with an input beam of $\sim 70 \times 120 \mu\text{m}$ FWHM. The results are similar to those of Fig. 1, with one important difference: because the modes are non-consecutive, their superposition does not possess transverse momentum. Consequently, a bimodal beam composed of non-consecutive modes is always propagating on-axis for any relative phase between its constituents. This is especially important when the beams are of high power (Fig. 2e and f): the trajectory of the self-trapped beam is always on-axis, irrespective of the relative phase (in contrast to Fig. 1e and f, which exhibited off-axis propagation). Consequently, when an ensemble average is taken over multiple random realizations of the relative phase, no statistical nonlinear diffraction occurs, and this ensemble-average self-trapped beam is a bimodal incoherent soliton.

EXPERIMENTS WITH HIGHLY MULTIMODAL BEAMS

We used a rotating diffuser to generate spatially incoherent light. The fluctuation time, t_c , of the spatially incoherent light is determined by the rotation rate of the diffuser. Such a light source is the monochromatic realization of a thermal source⁴³. We passed a broad laser beam through the diffuser, which was kept stationary during each temporal window, giving rise to a highly speckled beam. Passing the beam through the diffuser at different positions makes the population and phase of each of its modes vary randomly from one temporal window to the next. This multimode beam was imaged (demagnified) onto the input face of the sample. We monitored the input and output intensity structure at each of the individual time windows, after the thermal nonlinearity had reached steady state. Finally, we computed the ensemble-average intensity by averaging over all realizations.

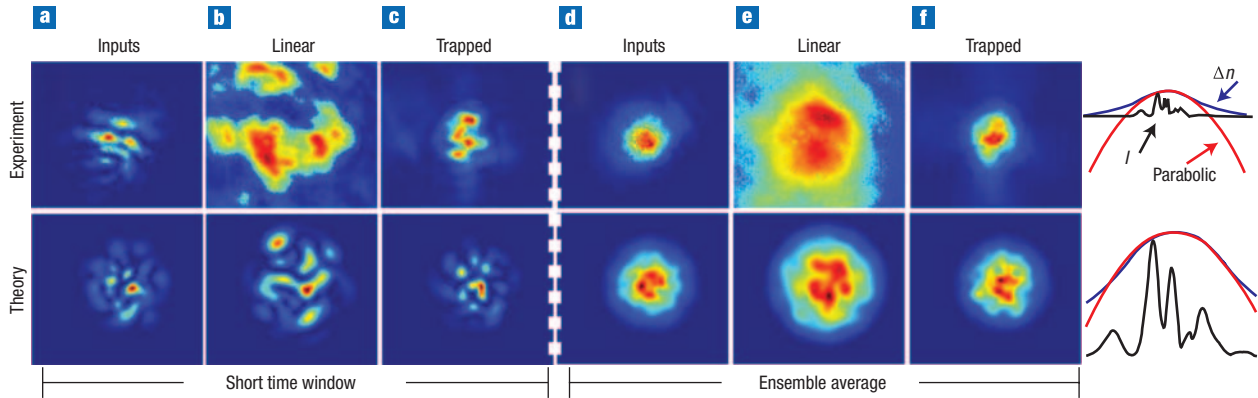


Figure 3 Incoherent solitons in effectively instantaneous nonlocal, nonlinear media. **a–c**, One typical realization of the highly multimode beam: input (**a**), output after linear diffraction at low power (**b**), and self-trapped output at high power (**c**). **d–f**, Self-trapping of the ensemble-average beam (taken over 50 random realizations): input (**d**), output after linear diffraction at low power (**e**), output forming an incoherent soliton at high power (**f**). The panel on the top right, and the enlargement below it, show that the calculated refractive-index change Δn in our medium (blue line) coincides with a parabolic shape (red line), in all regions of non-negligible optical intensity, I (black line). The dimensions of these plots are $1,140 \mu\text{m} \times 900 \mu\text{m}$.

To facilitate a quantitative comparison between the input and the output beams, for both the instantaneous case and the ensemble-averaged case, we had to evaluate their width and average speckle size (the latter determining the transverse correlation distance upon the incoherent beams, which is dependent on the modal population). Consider first the self-trapped multimode beam within a particular time window i . This is a speckled beam, so one cannot define its width as the FWHM. Instead, we define the effective width of such a beam as $d_i = [(\int \int I_i dx dy)^2 / (\int \int I_i^2 dx dy)]^{1/2}$. For a self-trapped multimode beam, the effective width should be stationary during propagation, although the actual intensity structure varies with propagation due to modal beating. In addition to the effective width, we define w_i , the average speckle-size of each self-trapped multimode beam, as the inverse of the FWHM of the spatial power spectrum (Fourier transform) of the beam. The comparison between input and output instantaneously self-trapped beams should be made through their effective width and average speckle size. Similarly, for the ensemble-averaged beams we defined the mean effective width $\langle d \rangle = 1/N \sum_{i=1}^N d_i$ and mean speckle size $\langle w \rangle = 1/N \sum_{i=1}^N w_i$. To prove an incoherent soliton, it is essential to compare the mean-effective width $\langle d \rangle$ with the width of the ensemble-average intensity structure $\bar{d} = d(\langle I \rangle)$, and find the standard deviation

$$\sigma = \sqrt{\langle d \rangle^2 - \bar{d}^2}.$$

In this sense, $\sigma \rightarrow 0$ indicates that the statistical nonlinear diffraction is negligible and we have an incoherent soliton.

Our experiments with highly multimode beams are presented in Fig. 3. Figure 3a shows one typical realization of the highly speckled input beam with $d \sim 175 \mu\text{m}$ and $w = 35 \mu\text{m}$. At low power, the beam diffracts and the output beam is broad (Fig. 3b), with $d \sim 570 \mu\text{m}$ and $w = 91 \mu\text{m}$. At high power, the speckled beam self-traps (Fig. 3c), with $d \sim 190 \mu\text{m}$ and $w = 37 \mu\text{m}$. The fine details of each self-trapped output beam are different from those of its corresponding input beam due to modal beating. However, the trajectory of each beam is on-axis, because the contribution of the interference between consecutive modes to the structure of the beam is small. We therefore expect

that the statistical nonlinear diffraction of the ensemble-average beam to be negligible. Indeed, Fig. 3d–f show that the ensemble-average beam conserves its effective width and its correlation distance (average speckle size), with $\sigma \rightarrow 0$. That is, not only did the instantaneous speckled beams self-trap within each time window, but the ensemble-average, highly multimode beam displays stationary propagation, forming an incoherent soliton.

It is now instructive to discuss the parameters defining the average speckle size (transverse correlation distance) of such an incoherent soliton. The average speckle size depends on two parameters: the beam power (defining the depth and width of the induced waveguide) and the specific statistic of the input beam (defining the modal population within the incoherent soliton). The statistics of the input beam is fixed for a given light source; the average speckle size of the incoherent soliton will consequently depend solely on the beam power, as we always use the same source. We can therefore construct an ‘existence curve’ for the incoherent soliton, relating its average speckle size and its power. Experimentally, we generate incoherent solitons at various power levels, use the same diffuser setting, but scale the demagnification such that the ratio between the effective width of each input beam and its speckle size, d/w , is fixed for every power level. The results are shown in Fig. 4. The theoretical curve is calculated for a gaussian modal distribution, as described in the Methods. Clearly, the experiments conform nicely to the theory.

DISCUSSION

We note that the induced waveguide in our system, $\Delta n(x, y)$, is approximately parabolic (wherever the beam intensity is not vanishingly small). As such, the modes $\psi_{l,m}(x, y)$ are approximately Gauss–Hermite modes (as experimentally proven in ref. 39). So, statistical nonlinear diffraction in x results from interference between modes (l, m) and $(l \pm 1, m)$ only, and statistical nonlinear diffraction in y results from interference between modes (l, m) and $(l, m \pm 1)$ (ref. 20). Consequently, the beam does not exhibit any noticeable deflection when many modes are populated within it, because the contribution of consecutive modes to the total transverse momentum is very small. These effects are highlighted in Figs 1 and 2 where the bimodal beam composed of modes 0 and 1 has the most apparent deflection, whereas the beam made

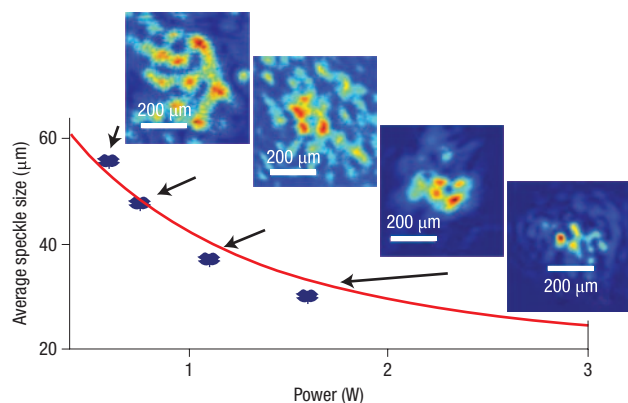


Figure 4 Existence curve of incoherent solitons in instantaneous nonlocal media. The figure shows the average speckle size of the incoherent soliton as a function of the total power of the beam for a given (quasi-thermal) light source setting the modal population. Each of the photographs displays one typical realization of a self-trapped speckled beam (comprising the incoherent beam) at a given power level. As the power increases, the self-trapped speckled beam narrows.

up of modes 0 and 2 does not exhibit deflection at all. Most importantly, Fig. 3 shows that the random deflection is negligible when many modes are present (this is likely to be the case for any highly nonlocal nonlinearity through which a symmetric bell-shaped potential is induced). That is, not only did the instantaneous speckled beams self-trap within each time window, but the ensemble-average highly multimode beam displays stationary propagation, forming an incoherent soliton.

Let us now discuss the intuitive meaning of the existence curve of Fig. 4. As the total power of the soliton beam increases, the width of the induced potential narrows and the potential becomes deeper, yet it always remains almost ideally parabolic (in the regions where the intensity is non-negligible). This means that the guided modes always retain the same structure (Gauss–Hermite-like). However, the modes of the deeper potential are narrower (more localized), and so are their interference patterns (the speckles). In other words, as the soliton becomes narrower, so do the speckles within it, which makes the diffraction effects stronger, forcing an asymptotically narrowing existence curve.

To conclude, we have demonstrated experimentally incoherent solitons in effectively instantaneous nonlocal, nonlinear media. We proved a new concept, that nonlocal nonlinearity can support incoherent solitons even when the response time of the nonlinearity is much faster than the fluctuation time²⁰. Our experiments demonstrate that highly fragmented coherent beams can be self-trapped. We foresee such experiments in materials where the nonlinearity is highly nonlocal yet very fast (of the order of picoseconds). Our experiments suggest the possibility of imaging through highly nonlocal, nonlinear media of the self-focusing type. Imaging through nonlinear media has always been a challenge⁴⁴, because the optical field evolves dynamically, in an intractable and irreversible fashion. For example, in Kerr media, which are represented by the (integrable) cubic nonlinear Schrödinger equation, the input field is projected onto a set of solitons and a continuum of radiation waves⁴⁵. The solitons evolve dynamically but their propagation is tractable through inverse scattering. However, the radiation waves, being extended states, carry information away to ‘infinity’ (physically, to the boundaries of the nonlinear sample, where radiation waves are lost). This

makes the problem irreversible due to loss of information. In contradistinction to nonlinear Kerr media and to all local optical nonlinearities, in a highly nonlocal, nonlinear medium, radiation waves (extended states) are absent⁴⁶, and as demonstrated here, all initially localized waves remain localized throughout propagation. Hence, the information content of the dynamically evolving optical field is conserved throughout propagation, and the problem of recovering that information is now reversible. Last but not least, we note that recent ideas with polar Bose–Einstein condensates and cold molecules predict a highly nonlocal, nonlinear response³⁰, which suggests the exciting possibility of implementing the ideas presented here with matter waves⁴⁷.

METHODS

THEORY

A linearly polarized, partially spatially incoherent beam can be described by its slowly varying amplitude $\Psi(x, y, z, t)$. When such a beam is self-trapped in a nonlinear medium (or guided in a waveguide), it is constructed from the eigenmodes of the system, which are determined by the potential (fixed, as in a waveguide, or induced by the nonlinearity), and the boundary conditions. As such, $\Psi(x, y, z, t)$ can be written as a superposition of its modal constituents ψ_n ,

$$\Psi(x, y, z, t) = \sum_n \sqrt{P_n(t)} \psi_n(x, y, z) \exp(i\varphi_n(t)). \quad (1)$$

The fluctuations in the modal power $P_n(t)$ and the modal phases $\varphi_n(t)$, which are what make the beam spatially incoherent, indicate many random realizations of the multimode beam appearing in each short time window ($\tau \ll t_c$), within which P and φ are constants. Thus, within each such time window, the modes ψ_n interfere, and Ψ is a coherent speckled beam. On the other hand, from one short time window to the next, P and φ change abruptly, switching from one speckled realization to another, in a random fashion. To stay within paraxiality, the characteristic speckle-size (approximately the transverse correlation distance) is much larger than the wavelength. Accordingly, within each short time frame, ψ_n evolves according to

$$(\partial_x^2 + \partial_y^2) \psi_n + 2ik\partial_z \psi_n + 2k^2(\Delta n/n_0) \psi_n = 0 \quad (2)$$

where $k = \omega n_0/c$, ω is the frequency, n_0 is the background refractive index, c is the speed of light in vacuum, and Δn is the induced index change ($|\Delta n| \ll n_0$). We used the highly nonlocal thermal nonlinearity of lead-glass, where Δn is proportional to the temperature change²⁴. In every time window of duration t_c , the beam experiences small absorption, thereby generating heat, which diffuses with time constant τ . If the duration of the time window is much larger than the response time ($\tau \ll t_c$), we neglect transients, and consider only Δn at the steady state, which satisfies the (time-independent) Poisson equation^{48,49} within that time window

$$\nabla^2 \Delta n(x, y, z, t) = -\bar{\kappa} |\Psi(x, y, z, t)|^2 \quad \text{for } t_i < t < (t_i + t_c) \quad (3)$$

where $\bar{\kappa}$ is a constant of the medium²². The nonlocality range in such nonlinearity is the actual size of the sample, which is much broader than the width of the beam^{22,23}. Consequently, to within a good approximation (which will be tested below), Δn depends on the total power of the beam $P = \sum_n P_n$, and not on its speckled structure. Moreover, the guided modes of Δn are approximately Gauss–Hermite polynomials³⁹. As these modes span all possible solutions of the paraxial wave equation, any realization of the incoherent beam can be guided under proper conditions.

We now find the modal structure of the waveguide induced by the speckled beam within a given time window. To do that, we first neglect the modal beating and use

$$\begin{aligned} |\Psi(x, y, z)|^2 &= \left| \sum_n \sqrt{P_n(t)} \psi_n(x, y, z, t) \exp(i\varphi_n(t)) \right|^2 \\ &= \sum_n P_n(t) |\psi_n(x, y, z)|^2 \end{aligned} \quad (4)$$

Under this assumption, we seek self-trapped solutions where $|\Psi|^2$ and Δn are z -independent. To do that, we substitute the expression of equation (4) in

equation (3), and solve equation (2) coupled to equation (3), self-consistently^{20,50}. That is, we find the modes $\psi_n(x, y, z) = \psi_n(x, y)\exp(-i\beta_n z)$ of the waveguide induced by $|\Psi|^2$. [We note that the modes we find deviate slightly from Gauss–Hermite modes, because Δn is never fully parabolic; nevertheless, the set of modes serves as an orthogonal basis for the solutions of the nonlinear wave equation].

Having found the set of modes $\{\psi_n(x, y)\}$ along with their propagation constants $\{\beta_n\}$, we can now simulate the propagation of a speckled beam containing a random superposition of modes, as represented by equation (1). We first recall our initial assumption that modal beating does not play any role in the structure of Δn . If this assumption is indeed correct, then launching the coherent speckled beam $\Psi(x, y, z = 0)$, within any particular time window (any realization of modal power distribution and modal phases), would yield self-trapped propagation, as long as the total power is unchanged. To prove this point, we simulate the propagation of 50 different realizations of $\Psi(x, y, z = 0)$, composed of the first 50 modes of Δn . Numerically, we use the standard split-step beam propagation method to solve equation (2), and use equation (3) to find the index change Δn from one propagation step to the next. We emphasize that, because the beam is fully coherent within the time window, the modes comprising it interfere and display modal beating. Nevertheless, all realizations of the coherent speckled beam are self-trapped, irrespective of the modal phases and modal power. That is, the intensity structure of the speckled beam, $|\Psi|^2$, is self-trapped: not exhibiting any diffraction broadening, in spite of the fact that the modes interfere with each other, resulting in an intensity structure that oscillates during propagation. The different realizations of the speckled beam do make one important difference in determining the induced waveguide: they determine the trajectory of Δn . In other words, the relative phases and power distribution among all the modes comprising Ψ determine the initial transverse momentum carried by the beam²⁰. Because the system conserves transverse momentum (when the beam is very far away from the sample boundaries⁴⁹), every realization yields a different trajectory of the instantaneous self-trapped speckled beam.

After establishing the features of the speckled self-trapped beams within each short (instantaneous) time window, we examine the long-timescale propagation. Looking at the incoherent beam at such $t \gg t_c$ is fully equivalent to taking an ensemble average over many possible realizations of these self-trapped randomly deflected beams. Because of the modal beating highlighted by Fig. 1, the ensemble-average propagation of the beam composed of consecutive modes 0 and 1 is not stationary, but rather exhibits statistical nonlinear diffraction. However, in the 50-mode beam of Fig. 3, the ratio of consecutive pairs to inconsecutive pairs is very small, hence its statistical nonlinear diffraction is negligible. When this happens, the ensemble average over all instantaneous self-trapped beams is stationary throughout propagation, forming an incoherent soliton.

Finally, we study the existence curve of these solitons (Fig. 4) by measuring the relation between the total power of the beam and the average speckle size of the soliton. Numerically, for each different power level, we find the set of modes $\{\psi_n(x, y)\}$ as described above. Recall that to construct the existence curve it is essential to have the same modal distribution (albeit at different widths) at all power levels. To conform with light emitted from a rotating diffuser (quasi-thermal source), we constructed the incoherent beam from a gaussian distribution of the first 50 modes $\langle P_n \rangle = P \exp(-n/\Delta) / \sum_{n=0}^{49} \exp(-n/\Delta)$ with $\Delta = 25$. The numerical results are compared to the experiment in Fig. 4.

Received 4 February 2008; accepted 16 April 2008; published 25 May 2008.

References

1. Stegeman, G. I. & Segev, M. Optical spatial solitons and their interactions: Universality and diversity. *Science* **286**, 1518–1523 (1999).
2. Mitchell, M., Chen, Z., Shih, M. & Segev, M. Self-trapping of partially spatially incoherent light. *Phys. Rev. Lett.* **77**, 490–493 (1996).
3. Mitchell, M. & Segev, M. Self-trapping of incoherent white light. *Nature* **387**, 880–883 (1997).
4. Chen, Z. *et al.* Self-trapping of dark incoherent light beams. *Science* **280**, 889–892 (1998).
5. Peccianti, M. & Assanto, G. Incoherent spatial solitary waves in nematic liquid crystals. *Opt. Lett.* **26**, 1791–1793 (2001).
6. Buljan, H. *et al.* Random-phase solitons in nonlinear periodic lattices. *Phys. Rev. Lett.* **92**, 223901 (2004).
7. Cohen, O. *et al.* Observation of random-phase lattice solitons. *Nature* **433**, 500–503 (2005).
8. Soljacic, M. *et al.* Modulation instability of incoherent beams in noninstantaneous nonlinear media. *Phys. Rev. Lett.* **84**, 467–470 (2000).
9. Kip, D., Soljacic, M., Segev, M., Eugenieva, E. & Christodoulides, D. N. Modulation instability and pattern formation in spatially incoherent light beams. *Science* **290**, 495–498 (2000).

10. Buljan, H., Šiber, A., Soljacic, M. & Segev, M. Propagation of incoherent ‘white’ light and modulation instability in noninstantaneous nonlinear media. *Phys. Rev. E* **66**, 035601 (2002).
11. Schwartz, T., Carmon, T., Buljan, H. & Segev, M. Spontaneous pattern formation with incoherent white light. *Phys. Rev. Lett.* **93**, 223901 (2004).
12. Buljan, H., Segev, M. & Vardi, A. Incoherent matter-wave solitons and pairing instability in an attractively interacting Bose–Einstein condensate. *Phys. Rev. Lett.* **95**, 180401 (2005).
13. Wu, M., Krivosik, P., Kalinikos, B. A. & Patton, C. E. Random generation of coherent solitary waves from incoherent waves. *Phys. Rev. Lett.* **96**, 227202 (2006).
14. Hasegawa, A. Dynamics of an ensemble of plane waves in nonlinear dispersive media. *Phys. Fluids* **18**, 77–78 (1975).
15. Mitchell, M., Segev, M., Coskun, T. H. & Christodoulides, D. N. Theory of self-trapped spatially incoherent light beams. *Phys. Rev. Lett.* **79**, 4990–4993 (1997).
16. Christodoulides, D. N., Coskun, T. H., Mitchell, M. & Segev, M. Theory of incoherent self-focusing in biased photorefractive media. *Phys. Rev. Lett.* **78**, 646–649 (1997).
17. Snyder, A. W. & Mitchell, D. J. Big incoherent solitons. *Phys. Rev. Lett.* **80**, 1422–1424 (1998).
18. Shkunov, V. V. & Anderson, D. Z. Radiation transfer model of self-trapping spatially incoherent radiation by nonlinear media. *Phys. Rev. Lett.* **81**, 2683–2686 (1998).
19. Buljan, H., Segev, M., Soljacic, M., Efremidis, N. N. & Christodoulides, D. N. White-light solitons. *Opt. Lett.* **28**, 1239–1241 (2003).
20. Cohen, O., Buljan, H., Schwartz, T., Fleischer, J. W. & Segev, M. Incoherent solitons in instantaneous nonlocal nonlinear media. *Phys. Rev. E* **73**, 015601 (2006).
21. Ulanir, E. A., Stegeman, G. I., Michaelis, D., Lange, C. H. & Lederer, F. Stable dissipative solitons in semiconductor optical amplifiers. *Phys. Rev. Lett.* **90**, 253903 (2003).
22. Rotschild, C., Cohen, O., Manela, O., Segev, M. & Carmon, T. Solitons in nonlinear media with an infinite range of nonlocality: First observation of coherent elliptic solitons and of vortex-ring solitons. *Phys. Rev. Lett.* **95**, 213904 (2005).
23. Rotschild, C., Alfassi, B., Cohen, O. & Segev, M. Long-range interactions between optical solitons. *Nature Phys.* **2**, 769–774 (2006).
24. Dabby, F. W. & Whinnery, J. R. Thermal self-focusing of laser beams in lead glasses. *Appl. Phys. Lett.* **13**, 284–286 (1968).
25. Litvak, A. G. Self-focusing of powerful light beams by thermal effects. *JETP Lett.* **4**, 230–233 (1966).
26. Suter, D. & Blasberg, T. Stabilization of transverse solitary waves by a nonlocal response of the nonlinear medium. *Phys. Rev. A* **48**, 4583–4587 (1993).
27. Segev, M., Crosignani, B., Yariv, A. & Fischer, B. Spatial solitons in photorefractive media. *Phys. Rev. Lett.* **68**, 923–926 (1992).
28. Conti, C., Peccianti, M. & Assanto, G. Route to nonlocality and observation of accessible solitons. *Phys. Rev. Lett.* **91**, 073901 (2003).
29. Conti, C., Peccianti, M. & Assanto, G. Observation of optical spatial solitons in a highly nonlocal medium. *Phys. Rev. Lett.* **92**, 113902 (2004).
30. Griesmaier, A., Werner, J., Hensler, S., Stuhler, J. & Pfau, T. Bose–Einstein condensation of chromium. *Phys. Rev. Lett.* **94**, 160401 (2005).
31. Lahaye, T. *et al.* Stabilization of a purely dipolar quantum gas against collapse. *Nature* **448**, 672–675 (2007).
32. Pecseli, H. L. & Rasmussen, J. J. Nonlinear electron waves in strongly magnetized plasmas. *Plasma Phys.* **22**, 421–438 (1980).
33. Rao, N. N. & Shukla, P. K. Triple-hump upper-hybrid solitons. *Phys. Scripta.* **T82**, 53–59 (1999).
34. Litvak, A. G., Mironov, V. A., Fraiman, G. M. & Yunakovskii, A. D. Thermal self-effect of wave beams in a plasma with a nonlocal nonlinearity. *Fiz. Plazmy* **1**, 60–71 (1975).
35. Turitsyn, S. K. Spatial dispersion of nonlinearity and stability of multidimensional solitons. *Theor. Math. Phys.* **64**, 226–232 (1985).
36. Krolkowski, W. & Bang, O. Solitons in nonlocal nonlinear media: Exact solutions. *Phys. Rev. E* **63**, 016610 (2000).
37. Xu, Z., Kartashov, Y. V. & Torner, L. Upper threshold for stability of multipole-mode solitons in nonlocal nonlinear media. *Opt. Lett.* **30**, 3171–3173 (2005).
38. Hutsebaut, X., Cambourac, C., Haelterman, M., Adamski, A. & Neyts, K. Single-component higher-order mode solitons in liquid crystals. *Opt. Commun.* **233**, 211–217 (2004).
39. Rotschild, C. *et al.* Two-dimensional multipole solitons in nonlocal nonlinear media. *Opt. Lett.* **31**, 3312–3314 (2006).
40. Snyder, A. W. & Mitchell, D. J. Accessible solitons. *Science* **276**, 1538–1541 (1997).
41. Mandel, L. & Wolf, E. *Optical Coherence and Quantum Optics* (Cambridge Univ. Press, 1995).
42. Mitchell, M., Segev, M. D. & Christodoulides, N. Observation of multihump multimode solitons. *Phys. Rev. Lett.* **80**, 4657–4660 (1998).
43. Bertolotti, M., Daino, B., Gori, F. & Sette, D. Coherence properties of a laser beam. *Nuov. Cim.* **38**, 1505–1514 (1965).
44. Kip, D., Anastassion, C., Eugenieva, E. & Christodoulides, D. N. Transmission of images through highly nonlinear media by gradient-index lenses formed by incoherent solitons. *Opt. Lett.* **26**, 524–526 (2001).
45. Ablowitz, M. J. & Segur, H. *Solitons and the Inverse Scattering Transform* (Society for Industrial and Applied Mathematics, Philadelphia, PA, 1981).
46. Kaminer, I., Rotschild, C., Manela, O. & Segev, M. Periodic solitons in nonlocal nonlinear media. *Opt. Lett.* **32**, 3209–3211 (2007).
47. Tikhonenkov, I., Malomed, B. A. & Vardi, A. Anisotropic solitons in dipolar Bose–Einstein condensates. *Phys. Rev. Lett.* **100**, 090406 (2008).
48. Iturbe-Castillo, M. D., Sánchez-Mondragón, J. J. & Stepanov, S. Formation of steady-state cylindrical thermal lenses in dark stripes. *Opt. Lett.* **21**, 1622–1624 (1996).
49. Alfassi, B., Rotschild, C., Manela, O., Christodoulides, D. N. & Segev, M. Boundary force effects extracted on solitons in nonlinear media with a very large range of nonlocality. *Opt. Lett.* **32**, 154–156 (2007).
50. Snyder, A. W., Mitchell, D. J., Poladian, L. & Ladouceur, F. Self-induced optical fibers: Spatial solitary waves. *Opt. Lett.* **16**, 21–23 (1991).

Acknowledgements

This work was supported by the Israeli Science Foundation. C.R. gratefully acknowledges the generous support of the ADAMS fellowship of the Israeli Academy of Arts and Sciences.

Author information

Reprints and permission information is available online at <http://npg.nature.com/reprintsandpermissions/>. Correspondence and requests for materials should be addressed to M.S.